Decadal Water Mass Variations Along 20°W in the Northeastern Atlantic Ocean

Gregory C. Johnson [a, *] and Nicolas Gruber [b]

[1] *NOAA/Pacific Marine Environmental Laboratory, 7600 Sand Point Way Bldg. 3, Seattle Washington 98115-6349, U.S.A*

[b] *Institute of Geophysics and Planetary Physics & Department of Atmospheric and Oceanic Sciences, University of California Los Angeles, Los Angeles California 90095-1567, U.S.A.*

Submitted to Progress in Oceanography 25 February 2005

Revised 8 September 2005

Abstract

Water mass variations in the northeastern Atlantic Ocean along 20°W are analyzed with pentadal resolution over the past 15 years using data from four repeat occupations of a meridional hydrographic section running south from Iceland. The section was sampled in 1988, 1993, 1998, and 2003. The results are interpreted in the context of changes in air-sea forcing, ocean circulation, and water properties associated with the North Atlantic Oscillation (NAO). The NAO index oscillated around zero from 1984–1988, was strongly positive from 1989–1995, after which it shifted to lower positive, and occasionally negative values from 1996–2003. Previously published studies suggest that after the 1995/1996 shift of the NAO, the subpolar gyre

[*]Corresponding author. Tel.: +1-206-526-6806; fax: +1-206-526-6744.
E-mail address: gregory.c.johnson@noaa.gov (G. C. Johnson).

largely retreated to the northwest in the northeastern Atlantic Ocean, resulting in an increasingly southeastern character of local water masses with time. Water property changes extending from the SubPolar Mode Water (SPMW) just below the seasonal pycnocline through the density range shared by Mediterranean Outflow Water (MOW) and SubArctic Intermediate Water (SAIW) along 20°W are consistent with changes in wind-driven ocean circulation and air-sea heat flux associated with shifts in the NAO, especially after accounting for ocean memory. After periods of lower NAO index the SPMW is warmer, saltier, and lighter. At these same times, large increases of Apparent Oxygen Utilization (AOU) and potential vorticity (Q) are found at the SPMW base, consistent with SPMW ventilation to lighter densities during lower NAO index periods. Deeper and denser in the water column, the cold, fresh, and dense SAIW signature within the permanent pycnocline that was most strongly present in 1993, near the culmination of a period of high NAO index, is much reduced in 1988 and 1998. In 2003, after a prolonged period of lower NAO index, increasing influence of warmer, saltier subtropical waters is clear within the permanent pycnocline. The deep penetration of the changes implies that they are caused primarily by circulation changes resulting from NAO associated wind shifts, but changes in air-sea heat flux could also have played a role.

Keywords: Dissolved Oxygen; Heat Storage; Ocean-Atmosphere System; Ocean Circulation; Temporal Variations; Water Masses; Eastern Subpolar North Atlantic Ocean

1. Introduction

The subpolar gyre of the North Atlantic Ocean has a rich water-mass structure that exhibits significant spatial and temporal variability. We describe recent water-mass variability in the eastern part of that gyre, focusing primarily on changes from the base of the seasonal pycnocline to the base of the permanent pycnocline, starting with the SubPolar Mode Water (SPMW) and extending down through the density range of the Mediterranean Outflow Water (MOW) and SubArctic Intermediate Water (SAIW). The analysis here uses data from hydrographic sections repeatedly sampled along 20°W every 5 years between 1988 and 2003. As shown by the following brief review, similar changes using subsets of the water mass signatures analyzed here have been documented extensively for the 1990's in the scientific literature using other data sets. Previous work also relates these variations to changes in the large-scale climate of the region around the North Atlantic Ocean.

SPMW is a convectively formed water mass, marked by a pronounced thermostad (a region of reduced vertical temperature gradient) as warm as 10–15°C in the eastern subtropical gyre (McCartney & Talley, 1982). In the subpolar gyre, this thermostad cools progressively from 8–10°C within the North Atlantic Current off Ireland to below 3.5°C in the Labrador Sea, following the cyclonic path of the gyre. The SPMW within the Labrador Sea has such an extreme expression as to warrant a separate name: Labrador Sea Water (LSW). Here the focus is on SPMW observed along 20°W in the potential temperature range of $6 < \theta < 14$°C between about 40°N and Iceland.

SPMW is embedded within, and comprises a large fraction of the central waters in the regional pycnocline (Paillet & Arhan, 1996a; 1996b; Pollard, Griffiths, Cunningham, Read,

Perez, & Rios, 1996; Pollard, Read, Holliday, & Leach, 2004). These pycnocline waters are often referred to as Western North Atlantic Water (WNAW) and Eastern North Atlantic Water (ENAW), depending on their properties and location in relation to the North Atlantic Current (NAC). WNAW is generally found west of the NAC, and is usually cooler, fresher, denser, and more stratified as compared with ENAW. WNAW is thought to gain its freshness and coolness in part from the influence of underlying SAIW that originates from the western boundary of the subpolar gyre (Pollard et al., 2004). In contrast, ENAW is thought to be saltier, warmer, and less stratified because it contains SPMW created by wintertime cooling, leading to deep mixed layers that are subducted within the eastern part of the North Atlantic.

SAIW is a cold fresh influence from the subpolar northwest that lies below the SPMW (Harvey & Arhan, 1988; Pollard et al., 1996; 2004) and Mediterranean Outflow Water (MOW) is a warmer, saltier influence from the subtropical southeast that lies near the same density levels as SAIW (Harvey & Arhan, 1988; Tsuchiya, Talley, & McCartney, 1992). While recent analyses (Potter and Lozier, 2004; González-Pola, Lavin, & Vargas-Yáñez, 2005) suggest that MOW water has become warmer and saltier in the North Atlantic, those changes are found closer to its source, well east of 20ºW. We will argue below those temporal variations in the SPMW properties observed along 20°W are consistent with changes observed at greater depth in the relative strengths of SAIW and MOW influences and thus circulation changes likely contribute to the observed water property variations.

The North Atlantic Oscillation (NAO) is a mode of atmospheric variability reflecting fluctuations between the Icelandic low and the Azores high, with a positive phase characterized by an anomalously high atmospheric pressure near the Azores and an anomalously low pressure near Iceland (Barnston & Livezey, 1987). NAO variations are linked to large-scale variations in

the air-sea fluxes of heat, freshwater, and momentum over much of the North Atlantic Ocean (Cayan, 1992; Hurrell, 1995; 1996; Visbeck, Cullen, Krahmann, & Naik, 1998; Marshall, Johnson, & Goodman, 2001). During periods of high NAO state, the subpolar gyre intensifies and expands to the southeast, and winter ocean heat loss over the gyre is also intensified. These circulation and air-sea heat flux variations can certainly have an effect on ocean water properties, including those of the SPMW. An extended winter (December–March) NAO index based on a principal component analysis of sea level pressure (downloaded from http://www.cgd.ucar.edu/cas/jhurrell/indices.html) oscillated around zero from 1984–1988, and then had an extended period of very high values from 1989–1995 before it shifted to lower positive, and occasionally negative, values from 1996– 2003 (Fig. 1, filled bars). The memory of the ocean circulation with regards to the effects of the NAO apparently can be approximated by an application of a backward-looking 9-year Blackman window and a 1-year lag (Fig. 1, solid line following Curry & McCartney, 2001) to this index. As noted by these authors, this filter mostly reflects the influence of conditions a few years previous, because of its weighting (see their Fig. 7d and associated discussion).

It has been argued that SPMW property variability is primarily owing to wind-driven shifts in circulation rather than local air-sea heat or freshwater fluxes (Pollard et al., 1996; 2004; Bersch, Meincke, & Sy, 1999; Bersch, 2002; Holliday, 2003). NAO shifts have been shown to change transport patterns throughout the North Atlantic (Curry & McCartney, 2001; Bersch, 2002) and advection of water properties by these changes appears important (Verbrugge & Reverdin, 2003). In the Northeastern Atlantic the 1995/1996 shift of the NAO index has been shown to be related to both changes in geostrophic currents estimated from hydrography and altimetry, and surface currents estimated from surface drifter and data wind-product derived

Ekman drifts, along with Sea-Surface Temperature (SST) data (Bersch, 2002; Flatau, Talley, & Niiler, 2003), as well as changes in eddy kinetic energy (often associated with changes in current locations) estimated from altimetry variability (Volkov, 2005). In this region, the shift from a high NAO state to low caused a northwestward shift in the NAC, hence a local contraction of the subpolar gyre. The contraction of this gyre allowed the invasion of warmer, saltier, and less stratified upper ocean waters there (Pollard et al., 1996; 2004; Bersch et al., 1999; Holliday, 2003).

However, the significant changes in buoyancy flux associated with NAO variability could also play a role in SPMW property changes, since a high NAO index is correlated with increased heat loss from the ocean to the atmosphere as far east as the region south of Iceland, as well as anomalous advection of cold surface water to the southeast in the surface Ekman layer (Marshall et al., 2001). Thus, a shift from positive NAO index to negative could be associated with warming SPMW due to changes in surface heat flux and Ekman transport, in addition to the effects gyre circulation changes owing to the time varying topographic Sverdrup balance.

2. Data

WOCE section A16N is a nominally meridional section that samples the deep eastern basins of the North Atlantic Ocean (Fig. 2; http://cchdo.ucsd.edu/). At least four occupations of the portion of this section between 20°N and Iceland have been made with closely spaced (55-km or closer intervals in the region studied except as noted below), full water column hydrographic stations with high-quality CTD (conductivity-temperature-depth) data and at least 24 nominal water samples per station. The first occupation analyzed here was in July–August

1988 on the *R/V Oceanus* (Tsuchiya et al., 1992). This section had one 100-km gap between about 59.4 and 60.3°N. The second occupation was in July–August 1993 on the NOAA Ship *Malcolm Baldrige* as part of the NOAA OACES program (with 110-km station spacing across most of the analysis region, but one 220-km gap between 33 and 35°N, another between 46 and 48°N, and 55-km spacing between 60 and 61°N). The third occupation was in April–June 1998 on the *RRS Discovery* (Smythe-Wright, 1998). The fourth occupation was in June–August 2003 on the NOAA Ship *Ronald H. Brown*, as the inaugural cruise of the U.S. Repeat Hydrography Program (http://ushydro.ucsd.edu/).

Full water column CTD temperature and salinity (S) data at 2-dbar pressure (P) intervals are analyzed from all four cruises. Temperature values are thought accurate to about ±0.002°C, salinity to about ±0.002 to ±0.005 (PSS-78) depending on the cruise, and pressure to about ±3 dbar. Potential temperature referenced to the surface (θ), potential density referenced to 1000 dbar (σ_1), and potential vorticity ($Q = f N^2/g$, where f is the Coriolis parameter, N the Brunt-Vaissala frequency, and g the acceleration of gravity) were all computed. Note that Q as estimated here neglects the contributions of relative vorticity, a reasonably approximation away from strong currents. The density parameter σ_1 was chosen because the study focuses on the upper 2000 dbar of the water column, and this quantity generally increases monotonically with increasing pressure throughout the water column. In contrast, potential density referenced to the surface exhibits large deep inversions in this region.

The 1988 and 2003 cruises report in situ oxygen sensor data at 2-dbar resolution that were calibrated using discrete bottle oxygen data. Oxygen were thought accurate to between ±1 and ±7 μ mol kg^{-1} (±0.5% and ±3%) depending on the cruise. For the 1993 and 1998 cruises, no oxygen sensor profiles were available, so discrete bottle oxygen data were linearly interpolated

to this resolution. For the 1993 cruise, the bottle oxygen data were multiplied by a factor of 1.02 after consultation with the chief scientist (R. Wanninkhof, 2004, personal communication). This adjustment likely brings the accuracy for the 1993 oxygen data nearer to those of the other cruises. AOU was computed by subtracting the measured value from the saturation value computed at θ and P = 0 using the solubility of Benson & Krausse (1984).

Profiles of θ, S, σ_1, and AOU were all low-passed in P with a 20-dbar half-width Hanning filter, and those of Q with a 80-dbar half-width Hanning filter. The results were then sub sampled at 20-dbar P intervals for isobaric analysis. For isopycnal analysis, the low-passed profile data (now excluding σ_1 but including P) were linearly interpolated to a set of finely spaced σ_1 values. For both analyses, vertical-meridional sections were contoured after objectively mapping the data onto a uniformly-spaced latitude grid at each level using a Gaussian correlation function and assuming a 2° latitude (221 km) decorrelation length-scale (this scale was doubled for the 1993 occupation, which had about twice the station spacing of the others) and a noise-to-signal energy ratio of 0.01. In addition to the maps, averages of ocean properties over latitude bands were made using the individual station data weighted by distances between stations.

The 5-year intervals between cruises may be aliased by interannual variations. To put the sections into a better resolved temporal context, satellite sea-surface height anomalies (SSHA) from a merged gridded product produced by AVISO containing data from multiple satellites (Ducet, Le Traon, & Reverdin, 2000) at monthly temporal and 1° spatial resolution were analyzed. Data spanned January 1993 through July 2004. The data were analyzed by first averaging SSHA in longitude from 25°W to 15°W for each month and 1° latitude gridpoint. This procedure resulted in a monthly SSHA time-series at each latitude in a 10°-longitude band

around 20°W. A time-mean, annual harmonic, and semiannual harmonic was fit to the time-series at each latitude. These components were removed from the time-series, and the resulting time-series were then each smoothed with a 1-year half-power point loess filter to highlight the interannual and longer time-scale variations in SSHA around 20°W.

3. Results

First we discuss the mean property fields using time-mean property sections analyzed along 20°W in pressure-latitude space and in potential density-latitude space. P is a more commonly used vertical coordinate than σ_1, and the isobaric analyses are useful for orienting the reader, as well as for estimating average values in a familiar vertical coordinate. However, heave of isopycnals, either from shorter time-scale eddy motions or longer time-scale gyre adjustments, can confuse isobaric analysis. Since water tends to flow along neutral density surfaces (here approximated by σ_1), isopycnal analysis tends to reduce mesoscale eddy noise in all property fields presented (except for P, where the full eddy signature is present), but if water mass densities vary spatially or temporally, that can complicate the analysis. Following the discussion of the mean water-mass signals, water property variations are analyzed using both vertical axes. In either vertical coordinate, averaging over large lateral extents, while necessary to reduce noise in estimates of temporal property variations, is not ideal because both pressure and density ranges of water masses can vary meridionally.

3.1. Time-mean water-mass properties along 20°W

Here we begin by describing the 1988-2003 average water mass properties of SPMW along the sections, located just below the seasonal pycnocline. We then progress deeper (and denser) in the water column through the permanent pycnocline to the MOW and SAIW. We only touch upon the LSW and northern deep overflow water mass properties.

3.1.1. SPMW properties

The very pronounced thermostads (Fig. 3a) of SPMW are visible between Iceland and about 40°N between the seasonal thermocline (about 200 dbar) and about 400–700 dbar, depending on the latitude. Between Iceland and the north slope of the Rockall Plateau (about 58°N), the thermostad has a temperature of 7–9°C and extends as deep as 700 dbar. It warms to 9–11°C and shoals to a maximum pressure around 400 dbar over the Plateau. Between the south slope of the Plateau (about 53°N) to about 40°N, it warms further to 10–13°C with a maximum pressure of about 600 dbar. South of 40°N the thermostad gradually fades and merges into the permanent thermocline. The SPMW thermostad is generally associated with relatively fresh mean S values (Fig. 3b), as expected in subpolar regions: the colder the thermostad, the fresher. Within the thermostad S starts just above 35.1 at the northernmost coldest extremes, and reaches about 35.8 in the warmest southernmost regions near 40°N.

SPMW is also a pycnostad as can be seen clearly by the vertical Q minimum (Fig. 4a) below the seasonal pycnocline. Like the thermostad, the Q minimum ($Q < 60 \times 10^{-12}$ m^{-1} s^{-1}) is quite strong and deep north of about 58°N, extending to about 700 dbar. Again, the Q minimum shoals to a maximum pressure of around 400 dbar above the Rockall Plateau, and from 40–53°N the Q minimum extends to about 600 dbar. South of 40°N the SPMW Q minimum values

increase and the minimum deepens and thins as it merges into the permanent pycnocline where stratified subtropical waters fill in above it. The parallels between the thermostad and the Q minimum are not surprising, since variations in θ are the dominant contributor to variations in density. These SPMW characteristics point to its formation in deep wintertime surface mixed layers.

The well-ventilated nature of SPMW is also evident in the mean AOU field (Fig. 4b). AOU within the SPMW is low, reflecting the relatively recent exposure of that water to the atmosphere. AOU within the SMPW ranges between 10 and 30 μmol kg^{-1} off Iceland, but values increase to the south, ranging between 30 and 60 μmol kg^{-1} by 40°N, likely caused by the oxygen consumption from the remineralization of organic matter as the water ages to the south. Remineralization rates most likely decrease with increasing depth and toward the south, complicating the interpretation. However, this aging is also evident in the increasing Q minimum values to the south. Even further south, both AOU and Q increase along the vestigial SPMW Q minimum.

The isopycnal spreading in the upper 700 dbar (Fig. 5a) directly reflects the presence of the SPMW Q minimum. Also of interest is the general tendency of isopycnals from the surface to at least 1600 dbar to rise to the north, implying increasingly eastward geostrophic velocities at shallower levels in the study region if a mid-depth level of low velocity is assumed. There is some variability about this trend. Relatively strong mean horizontal property gradients around 49–53°N and 57–61°N especially imply eastward flow in these regions, consistent with other maps of the regional circulation (Curry et al., 2001) and the various branches of the NAC (Pollard et al., 2004). In contrast, between these branches, from 53–57°N, isopycnals slope down to the north at least in the pressure range below the SPMW and above the Rockall Plateau,

consistent with the analyses just mentioned that indicate some northwestward component to the upper ocean flow in this latitude range at 20°W. The time-mean P of the isopycnals (Fig. 5b) is shown mainly as a reference for the isopycnal analysis. However, dynamic signatures are evident in it, but with reversed slopes as compared to the time-mean vertical-meridional section of σ_1 (Fig. 5a). That is to say, P values for about $\sigma_2 < 32.35$ kg m^{-3} generally get smaller to the north, as expected in the subpolar gyre.

Within the waters with $\theta > 11$°C ($\sigma_1 < 31.6$ kg m^{-3}), both θ (Fig. 6a) and S (Fig. 6b) are relatively constant on σ_1 surfaces and decrease steadily with increasing σ_1 across the latitude range analyzed. These are the central waters (Pollard et al., 2004). The distinctive Q minimum of SPMW (Fig. 7a) lies just within these central waters at density horizons as light as $\sigma_1 = 31.55$ kg m^{-3} at the southern end of the section, but going northward it is located at progressively denser horizons, becoming as dense as $\sigma_1 = 31.95$ kg m^{-3} just south of Iceland. The Q minimum stays within a 200–700 dbar range at all latitudes (Fig. 5b). The SPMW is also distinguished by its very low AOU values (Fig. 7b). Again, both low AOU and low Q are signatures of recent ventilation, and both reflect the origin of the SPMW, formed by deep winter convection within the surface mixed layer.

3.1.2. Permanent pycnocline properties

The permanent pycnocline underlies the SPMW, and can be characterized by a Q maximum that sits from 600–800 dbar (Fig. 4a) shallowest at about 53°N and deeper to the north and south along 20°W. Like the Q minimum of the SPMW above it, the density of the Q maximum increases to the north. It is located near $\sigma_1 = 31.85$ kg m^{-3} at and south of 40°N,

where its density begins increasing northward to about σ_1 = 32.15 kg m^{-3} off Iceland (Fig. 7a). The highest Q values are located at about 52°N. The decrease in the vertical Q maximum to the south is mostly owing to changes in the Coriolis parameter, with the maximum vertical stratification about constant at lower latitudes. To the north of 52°N, the Coriolis parameter increases slightly, so the strength of stratification within the permanent pycnocline actually declines there, as expected in the subpolar gyre.

Just below the Q maximum is an AOU maximum that is deeper by about 100 dbar (Fig. 4) and denser by about 0.1 kg m^{-3} (Fig. 7). This AOU maximum increases steadily to the south, most likely as a result of increasing ventilation time-scales in the subtropics, where the waters in the permanent pycnocline are well protected from ventilation and far removed from their source regions.

3.1.3. MOW and SAIW properties

MOW and SAIW are located just below the Q maximum of the permanent pycnocline, and are nearly vertically collocated with the associated AOU maximum. MOW and SAIW approximately share a density horizon, where the warm, salty MOW contrasts sharply with the much colder and fresher SAIW. MOW, that originates to the east in the warm, salty, dense overflow of Mediterranean Waters through the Strait of Gibraltar, is treated here as a deep marker of subtropical influence. SAIW, which originates in the western boundary current of the subpolar gyre and moves northeastward in the NAC (Pollard et al., 2004) is taken as a deep marker of subpolar influence.

The relatively deep thermostad centered from 10–11°C around 37°N is associated with the strong salinity maximum of MOW, centered at a pressure of about 1100 dbar (Fig. 3) and σ_1 = 32.15 kg m^{-3} (Fig. 6). SAIW can be roughly detected as a vertical minimum of S < 34.9 around θ of 6–7°C (Pollard et al., 2004). Water of this definition is not found in the mean sections, although SAIW influence certainly contributes to the general cooling and freshening north of the MOW. The freshest and coldest water (with S< 35.1) near σ_1 = 32.15 kg m^{-3} (strongest SAIW influence and subpolar gyre signature) is located around 53°N where the permanent pycnocline is shallowest (Fig. 5). The pycnocline shoaling there is also an indicator of subpolar influence, since isopycnals rise up towards the center of a subpolar gyre. A very strong meridional θ-S gradient from 40–45°N and around σ_1 = 32.15 kg m^{-3} (Fig. 6b) separates the warm salty MOW influence to the south from the cold fresh SAIW influence to the north.

Both the MOW, formed in an overflow, and the SAIW, originating in the western boundary current of the subpolar gyre, have relatively high Q, and high AOU. The AOU maximum is about 100 dbar deeper and 0.1 kg m^{-3} denser than the Q maximum of the permanent pycnocline (Figs. 4 and 7). The MOW salinity maximum (Figs. 3 and 6) is located less than 100 dbar below and 0.1 kg m^{-3} denser than the Q maximum. The lateral salinity minimum indicating the strongest SAIW influence is coincident in latitude with the absolute maximum values of Q in the mean section.

3.1.4. LSW and northern overflow properties

LSW lies below MOW and SAIW. LSW can be easily seen as a minimum in S (Figs. 3b and 6b), Q (Figs. 4 and 7), and AOU, as well as a thermostad in θ (Fig. 3a). These features are

located at about 1800 dbar and σ_1 = 32.4 kg m^{-3} in the mean. The LSW signature is strongest north of the Azores Biscay Rise, which is located at about 42°N. LSW variations along 20°W are analyzed elsewhere (Johnson et al., 2005).

The northern overflow waters from the Greenland-Iceland-Norwegian Seas that form a bottom boundary current just south of Iceland are another prominent deep feature at 20°W. They are relatively warm, salty, (Fig. 6) and high Q (Fig. 7a) compared with LSW. The high Q value is the signature of a highly stratified bottom-trapped overflow plume. In addition, the density field shows a strong signature of the boundary current, with isopycnals rising up towards Iceland, especially below 1400 dbar (Fig. 5), consistent with bottom-intensified westward geostrophic flow in the bottom boundary current.

These and other deeper water masses such as the abyssal waters of the eastern basin are not treated here. (See Tsuchiya et al., 1992 for a detailed description of all water masses as observed in the 1988 section and Harvey & Arhan, 1988 for analysis of data taken to the west of 20ºW.)

3.2. Water-mass property variability along 20°W

Again, the four sections allow for the determination of mean water properties over the analysis period (presented above) and deviations from this mean. In the following we attempt to put the deviations into a context by relating them to shifts in the NAO index as well as an integrated lagged version of the NAO index that has been shown (Curry & McCartney, 2001) to reflect the effects of ocean memory of and lagged ocean response to wind stress and buoyancy flux variations related to the NAO index primarily over the previous few years (Fig. 1).

Significant changes in upper ocean water properties along 20°W apparently related to NAO index shifts detailed below include generally warmer, saltier, and lighter SPMW following periods of lower NAO index, a pronounced increase in Q and AOU at the base of the SPMW probably related to the lighter character of the SPMW, and a decreased subpolar SAIW influence. These changes are discussed in both isobaric and isopycnal vertical coordinates. To limit the number of figures, only contour plots of differences between the 1993 and 2003 occupations are presented. These differences are usually the most dramatic since the former occupation is near the end of the 1989–1995 high NAO index period and the latter is well into a period of lower NAO index. The two-section differences are supported by analysis of some averages of water properties from all the sections made over selected latitude ranges.

The latter three cruises can also be put into context using SSHA data (Fig. 8), processed as described in Section 2. Low SSHA values along 20°W near the time of the 1993 cruise likely indicate the presence of cold, fresh, SPMW during the high NAO index period, with lowest values observed about a year after the 1993 section was occupied. Generally higher values are seen in the region a few years after the 1995/1996 NAO index shift, as expected from the lagged ocean response with westward and northward contraction of the subpolar gyre documented in the literature reviewed (e.g. Curry & McCartney, 2001) in the introduction. These higher values, presumably related to the northwestward spreading of warmer, lighter SPMW from the southeast, are coincident with the 1998 and 2003 data. While there is some interannual variation, the overall impression is of higher SSHA values found along 20°W after the 1995/1996 NAO index shift over decadal time-scales.

3.2.1 SPMW property variations

The difference of θ between 2003 and 1993 (Fig. 9a) as a function of latitude and pressure exhibits a pronounced warming throughout the pressure and latitude ranges of the SPMW that reaches peak local values of about 1.5°C. Mesoscale features are evident even in the differences of the laterally smoothed sections, but the sign of the decadal change stands clearly above the mesoscale. Averaged between 40°N and Iceland (Fig. 9b), the first two sections were colder than the last two, with 1993 (near the peak of the 1989–1995 high NAO index period) being the coldest, and 2003 (well into a lower NAO index period) being the warmest from the base of the seasonal thermocline (200 dbar) throughout the SPMW (600–800 dbar). The average warming between 1993 and 2003 north of 40°N is about 0.7°C from 300–600 dbar.

The colder and denser water seen in the upper 100 m the 1998 section (Fig. 9) is a seasonal effect because that section was occupied in earlier in the year than the other three sections. It is also possible that this seasonal sampling bias in the 1998 section influences SPMW properties by sampling SPMW closer to its formation time resulting in lower Q, AOU and θ (e.g. Reverdin, Assenbaum, & Prieur, 2005).

The SPMW warming is accompanied by increased salinities over the period of study with a local peak of over 0.2 in the SPMW between 1993 and 2003 (Fig. 9c). Averaged between 40°N and Iceland (Fig. 9d) the first two sections were fresher than the last two in the SMPW, again with 1993 being the freshest, and 2003 being the saltiest from the base of the seasonal thermocline (200 dbar) at least throughout the SPMW (600–800 dbar). The average salinification between 1993 and 2003 north of 40°N is about 0.1 from 300–600 dbar.

Temperature and salinity changes are positively correlated, as might be expected, but examination of σ_1 as a function of pressure and latitude shows that in general the effect of the

warming trend on density is not completely compensated by the associated salinification. In fact, σ_1 decreases almost everywhere within the region of SPMW between 1993 and 2003 (Fig. 9e). Averaged between 40°N and Iceland (Fig. 9f) the first two sections were denser than the last two in the SMPW, again with 1993 being the densest, and 2003 being the lightest overall in the SMPW The average decrease in σ_1 from 1993 to 2003 north of 40°N is about 0.05 kg m^{-3} from 300–600 dbar.

The variations of differences of θ between the 2003 and 1993 sections mapped on isopycnals (Fig. 10a) are relatively small compared with those on isobars, because the effects of isopycnal heave are removed in isopycnal analyses. In addition, since water that becomes warmer on a given isopycnal must also be saltier to remain on that isopycnal, the variations of S are not shown because they are redundant with those of θ. Variations of θ-S on isopycnals between 1993 and 2003 appear small within the central water (σ_1 < 31.6 kg m^{-3}), with θ differences being mostly less than 0.25°C (equivalent to about 0.05 in S) in either direction. However, within the SPMW, the θ-S relation is mostly warmer (by 0.25–0.5°C) and thus saltier (by about 0.05–0.11) in 2003 compared to 1993 north of about 45°N.

The general increased pressure of isopycnals between 1993 and 2003 within the SMPW ranges is striking (Fig. 10b). Vertical excursions are nearly everywhere positive in the upper portion of the water column, often more than 100 dbar in magnitude, and reaching 400 dbar in one location just south of Iceland. These changes are somewhat patchy laterally, probably owing to mesoscale variability from eddies current shifts. The overall deepening of isopycnals is consistent with the signature of lighter water on isobars within the SPMW after the 1995/1996 NAO index shift discussed above. Differences in θ-S and pressure of isopycnals within the

SMPW among the other sections (not shown) are all smaller than those between 2003 and 1993, but still consistent with the NAO index shifts.

3.2.2 Permanent pycnocline property variations

Variations within the areas of strong vertical density and AOU gradients may be owing to ventilation changes at the base of the SPMW which affect the permanent pycnocline, but could also originate from circulation changes which also alter the properties of the permanent pycnocline through advection. The most prominent changes in the pycnocline are manifest as variations in Q and AOU. Starting with Q differences on isobars (Fig. 11a) a large increase in Q between 1993 and 2003 is evident at the base of the SPMW, within the permanent pycnocline, at about 500–900 dbar. The difference fields are relatively noisy, as might be expected within a region of strong vertical gradients. Q differences are mostly positive in this pressure range and often exceed 40×10^{-12} m^{-1} s^{-1}. Variations in Q changes between these sections are strongly and positively correlated with AOU changes (Fig. 11b), with local AOU changes exceeding 30 μmol kg^{-1} in a few locations.

This positive correlation should not be too surprising, since low AOU and low Q are both signs of recent ventilation, and higher values of these properties indicate less recent ventilation or mixing with other water-masses (Jenkins, 1982). As the SPMW gets warmer, saltier, and lighter, Q and AOU just below the SPMW (500–900 dbar) also increase. These changes could be related to circulation changes associated with the 1995/1996 shift in the NAO moving SPWM of lower latitude origins subjective to less vigorous ventilation northward and westward (e.g. Curry & McCartney, 2001). They could also be due in part to reductions in local ventilation due

to reductions in local winter heat flux and Ekman-driven heat transports after the 1995/1996 shift (e.g. Marshall, Johnson, & Goodman, 2001). Averages of these properties between 40°N and Iceland and their deviations from the time-mean show that from 600–800 dbar, AOU increased by 16 μmol kg^{-1} (Fig. 11d) between 1993 and 2003, and Q increased by 20×10^{-12} m^{-1} s^{-1} (Fig. 11b). Generally low values in 1988 and intermediate values in 1998 are consistent with the hypothesis of water property changes induced by shifts in the NAO, caused by circulation changes, air-sea heat flux variations, or both. In 1993 there is also some indication of higher AOU and Q values within the upper portions of the SPMW than for other years, consistent with a more stratified western subpolar source of central waters (Pollard et al., 2004).

The differences in Q and AOU (Fig. 12) between 2003 and 1993 on isopycnals also show widespread and significantly correlated patterns at the base of the SPMW. The noise level is lower than in the isobaric analysis, in part because eddy noise has been reduced, and in part because the permanent pycnocline is deeper in 2003 compared with 1993, moving the relevant isopycnals into more stratified, less well-ventilated (hence higher AOU) higher pressures in 2003. The maximum differences for both quantities are located in the high vertical gradient region just below the SPMW, with a core from as light as $\sigma_1 = 31.6$ kg m^{-3} at 40°N to as dense as $\sigma_1 = 32.1$ kg m^{-3} off Iceland. In 1993, Q and AOU anomalies are negative in this region, as would be expected for more northwesterly waters. In 2003, both AOU and Q anomalies in this same region are increasingly positive, suggesting an invasion of lighter SPMW from the south and east after the 1995/1996 NAO shift. Again, the 1988 and 1998 sections (not shown) are consistent with driving by changes in the NAO, with low relatively Q and AOU in 1988, and intermediate values in 1998.

3.2.3. MOW and SAIW property variations

On the deeper and denser side of the Q maximum indicating the center of the permanent pycnocline, differences of θ (Fig. 9a) and S (Fig. 9c) on isobars between 1993 and 2003 document that even here water masses have become warmer and saltier, and somewhat lighter (Fig. 9e), especially between about 45°N and 58°N, where the SAIW influence was strong in 1993 but much lessened in 2003, as might be expected from a northwestward retraction of the NAC after the 1995/1996 NAO index shift. The isobaric averages of these quantities north of 40°N show significant warming and salinification, but almost completely density compensated, between 1988 and 2003 (Fig. 9b, d, and f). However, this latitude range was chosen primarily for looking at SMPW changes, and deeper down it includes the strong meridional gradient in the θ-S relation between the MOW and SAIW that exists from 40–45°N (Figs. 3 and 6). As a result, these averages are subject to aliasing by the presence or absence of mesoscale lenses containing MOW.

Isopycnal analysis (Fig. 10a) reveals large changes in the θ-S relation between 1993 and 2003 from about 45–55°N, throughout the permanent pycnocline, and peaking near the density shared by the MOW and SAIW, $\sigma_1 = 32.0$ kg m^{-3}. The isopycnal deepening between these two occupations over the same latitude and a wide density range frequently exceeds 100 dbar (Fig. 10b). This deepening is consistent with the θ-S variations, since shallower isopycnals are a signature of a strong subpolar gyre, the deepening is likely a signature of the retreat of that gyre to the north and west of 20°W, as might be expected during periods of lower NAO index (Curry et al., 2001; Bersch, 2002; Flatau et al., 2003). This region is north of the strong property gradient between MOW and SAIW. Pentadal variations in the isopycnally averaged θ-S relation

from 45–55°N (Fig. 13) reveal that the cold, fresh influence of SAIW peaked in 1993, near the end of the 1989-1995 period of high NAO index and was intermediate in 1988 and 1998, whereas a more southeastern warm, salty MOW influence was present deep in 2003, well into a period of lower NAO index.

4. Discussion.

The time-series analyzed here is consistent with previous findings in that SPMW along 20°W is colder, fresher, and denser in 1993, well into a prolonged period of high NAO index, and warmer, saltier, and lighter in the other sections, after periods of lower NAO index. The more recent data presented here show that this pattern persists and strengthens through mid-2003. During low NAO index periods, the lightening of SPWM is accompanied by a large increase in AOU and Q at the SPMW base. These changes and their relation to changes in buoyancy forcing are not thoroughly discussed in the literature for SPMW, but have been analyzed in a subtropical mode water (Jenkins, 1982). In that study, correlations among anomalously low ocean heat loss, increased Q, and increased AOU were presented. With lower heat loss, winter mixed layers do not become as dense, so AOU and Q can both increase with time on the denser horizons of the mode water during periods when these horizons are not ventilated.

The changes observed could be owing to local variations in buoyancy forcing, or has been argued above for the SPMW, circulation changes resulting from a shift in the NAC might also contribute. SMPW originating to the southeast of the NAC is ventilated on lighter density horizons with respect to that originating to the northwest of the NAC, so a northwestward shift in

the NAC would shift warmer, saltier, lighter SPWM with higher Q and AOU at lighter density horizons northwestward.

Below these maxima, a cold fresh SAIW signature of northwestern origin observed most strongly in the 1993 data is increasingly replaced by a warmer, saltier MOW influence from the southeast in later sections. These deeper water property changes are also consistent with a northwestward contraction of the subpolar gyre in this area after the 1995/1996 NAO shift. Unlike the SPMW, these water masses are not exposed directly to air-sea forcing via the winter mixed layer around 20°W. Thus, the consistency of the water-mass changes down through the permanent pycnocline is evidence that NAO-driven changes in circulation and advection may be the primary cause of SPMW variations, perhaps aided by NAO-related changes in air-sea buoyancy fluxes.

Below the SAIW and MOW is LSW. The variations of LSW are also related to changes in the NAO, but exist primarily owing to a different mechanism than subpolar gyre shifts. LSW property variations (e.g. Yashayaev, Lazier, & Clarke, 2003) arise primarily from variations in air-sea fluxes of heat and freshwater. These property variations take between years and a decade to spread around the deep subpolar gyre (Koltermann, Sokov, Tereschenkov, Dobroliubov, Lorbacher, & Sy, 1999). Variations in LSW properties observed along 20°W are analyzed elsewhere (Johnson, Bullister, & Gruber, 2005).

The analysis presented above suggests that from the base of the seasonal pycnocline down through the entire permanent pycnocline, water-mass properties exhibited large changes in the subpolar North Atlantic along 20°W between 1988 and 2003. This study adds to the literature through its analysis of water mass changes spanning the permanent pycnocline along 20°W, including recent 2003 information.

All of these results are consistent with a circulation change associated with the 1995/1996 shift in the NAO index from strongly positive to more neutral values (Curry et al., 2001; Bersch, 2002; Flatau et al., 2003). This NAO shift likely induces a reduction of subpolar influence along 20°W as the subpolar gyre retracts northward and westward (Pollard et al., 1996; 2004; Bersch et al., 1999). In addition, anomalous ocean heat flux and Ekman transport patterns associated with NAO index variability do extend east to the region south of Iceland (Marshall et al., 2001). These shifts would also act to warm SPWM after 1995. The deep changes in SAIW influence support the argument for primacy of a circulation change over the effects of surface buoyancy flux variations in driving SPMW properties and the associated increases in AOU and Q at the top of the permanent pycnocline. This argument is consistent with previous analyses in the literature (Holliday, 2003), but more analysis may be required to resolve fully this issue. We have emphasized NAO index variability here, because of the strength of that signal in the North Atlantic. However, a longer-term warming trend in the ocean (Levitus, Antonov, & Boyer, 2005) could also result in ventilation of lighter (and perhaps shallower) winter mixed layers with time. Such a trend might cause changes in the AOU (Keeling & Garcia, 2002) and Q fields similar to those observed here.

The tight correlation between AOU and Q in the subpolar North Atlantic along 20°W is interesting. Significant changes in subsurface oxygen concentration have been analyzed in other ocean basins. For instance, in the South Indian Ocean a substantial decrease in oxygen (increase in AOU) over decadal time-scales has been linked to a decrease in the strength of the subtropical gyre there (Bindoff & McDougall, 2000). As found in the North Atlantic, the increase in AOU in the Indian Ocean is associated with an increase in Q. Large decadal AOU changes have also been observed in the subpolar North Pacific Ocean (Emerson, Watanabe, Ono, & Mecking,

2004). These North Pacific oxygen changes have been linked to decadal variations in circulation and ventilation by model analyses (Deutsch, Emerson, & Thompson, 2005). AOU increases correlated with warming as observed in the eastern South Pacific Ocean have also been posited to result from decadal circulation variations there (Shaffer, Leth, Ulloa, Bendtsen, Daneri, Dellarossa, et al., 2000). Recently large AOU increases have also been observed the Southern Ocean south of Australia (M. Warner, personal communication 2004). It would be interesting to see if the AOU variations in the North Pacific, South Pacific, and Southern Oceans are also related to Q variability.

The AOU variations reported here and in other basins are fairly large and have significant implications for estimating the oceanic uptake of anthropogenic carbon. A 2 μmol kg^{-1} change in AOU corresponds to a 1.4 μmol kg^{-1} change in Dissolved Inorganic Carbon (DIC), somewhat larger than the annual increase in DIC expected in the mixed layer from the uptake of anthropogenic CO_2 from the atmosphere. These deep changes of up to 30 μmol kg^{-1} in AOU over a decade have associated DIC changes that exceed the anthropogenic signal at the surface over a decade, and thus need to be carefully evaluated in order to extract the smaller anthropogenic CO_2 signal. Given the corresponding changes in θ, S, σ_1, and Q, and the depth structure of the observed AOU changes, these AOU changes likely do not come from changes in the rate of biological oxygen demand (oxygen utilization rate, OUR) but are more likely a result of circulation changes, including a retracting subpolar gyre under low NAO index conditions, with a possible contribution from variations in air-sea buoyancy flux that may have reduced the density of winter ventilation.

Although a detailed investigation of these AOU changes is beyond the scope of this study, the discovery of such large trends in the oceanic oxygen content linked to variations in

transport and storage of heat and freshwater has substantial implications for understanding the global carbon cycle, as the atmosphere-ocean oxygen budget is commonly used to constrain the fate of the anthropogenic CO_2 emitted into the atmosphere (Keeling & Shertz, 1992; Keeling, Piper, & Heimann, 1996; Keeling et al., 2002). We need to recognize that a decadal, or in this case even a pentadal, sampling of a few sections in each ocean basin may not fully resolve the temporal and spatial evolution of the oxygen signals, resulting in a risk of aliasing changes that have potentially large impacts on biogeochemical budgets. Sub gyre-scale sampling of the ocean physical water property variations on seasonal time-scales afforded by the Argo Project global array of profiling CTD floats (Roemmich & Gould, 2003), together with a better understanding of the relation of AOU variations to those of physical water mass properties such as Q could help to put the biogeochemical data from the repeat hydrographic section into context.

Acknowledgments

The NOAA Office of Oceanic and Atmospheric Research further support GCJ and the National Science Foundation NG through a grant. The hard work of the officers, crew, and scientific personnel on all 4 occupations of WOCE section A16N is very gratefully acknowledged. The 2003 cruise was part of the NOAA/NSF Funded U.S. Repeat Hydrography Program in support of CO2 and CLIVAR. Constructive comments from two anonymous reviewers helped to improve the manuscript. This is Pacific Marine Environmental Laboratory contribution number 2792.

References

Barnston, A. G., & Livezey, R. E. (1987). Classification, seasonality, and persistence of low-frequency atmospheric circulation patterns. *Monthly Weather Review*, 115, 1083–1126.

Benson, B. B., & D. Krausse, D., Jr. (1984). The concentration and isotopic fractionation of oxygen dissolved in freshwater and seawater in equilibrium with the atmosphere. *Limnology and Oceanography*, 29, 620–632.

Bersch, M. (2002). North Atlantic Oscillation-induced changes of the upper layer circulation in the northern North Atlantic Ocean. *Journal of Geophysical Research*, 107, C10, 3156, doi:10.1029/2001JC000901.

Bersch, M., Meincke, J., & Sy, A. (1999). Interannual thermohaline changes in the northern North Atlantic 1991–1996. *Deep-Sea Research Part II*, 46, 55–75.

Bindoff, N. L., & McDougall, T. J. (2000). Decadal changes along and Indian Ocean section at 32°S and their interpretation. *Journal of Physical Oceanography*, 30, 1207–1222.

Cayan, D. R. (1992). Latent and sensible heat flux anomalies over the northern oceans: Driving the sea surface temperature. *Journal of Physical Oceanography*, 22, 859–881.

Curry, R. G., & McCartney, M. S. (2001). Ocean gyre circulation changes associated with the North Atlantic Oscillation. *Journal of Physical Oceanography*, 31, 3374–3400.

Deutsch, C., Emerson, S., & Thompson, L. (2005). Fingerprints of climate change in North Pacific oxygen. *Geophysical Research Letters*, 32, L16604, doi: 10.1029/2005GL023190.

Ducet, N, Le Traon, P.-Y., & Reverdin, G. (2000.) Global high-resolution mapping of ocean circulation from TOPEX/Poseidon and ERS-1 and -2. *Journal of Geophysical Research*, 105, C8, 19477-19498.

Emerson, S., Watanabe, Y. W., Ono, T., & Mecking, S. (2004). Temporal trends in apparent oxygen utilization in the upper pycnocline of the North Pacific: 1980–2000. *Journal of Oceanography*, 60, 139–147.

Flatau, M. K., Talley, L., & Niiler, P. P. (2003). The North Atlantic Oscillation, surface current velocities, and SST changes in the subpolar North Atlantic. *Journal of Climate*, 16, 2355–2369.

Harvey, J., & Arhan, M. (1988) The water masses of the central North Atlantic in 1983–84. *Journal of Physical Oceanography*, 18, 1855–1875.

Holliday, N. P. (2003). Air-sea interaction and circulation changes in the northeast Atlantic. *Journal of Geophysical Research*, 108, C8, 3259, doi: 10.1029/2002JC001344.

Hurrell, J. W. (1995). Decadal trends in the North Atlantic Oscillation: Regional temperatures and precipitation. *Science*, 269, 676–679.

Hurrell, J. W. (1996). Influences of variations in extratropical wintertime teleconnections on Northern Hemisphere temperature. *Geophysical Research Letters*, 23, 665–668.

Jenkins, W. J. (1982). On the climate of a subtropical ocean gyre: Decade time-scale variations in water mass renewal in the Sargasso Sea. *Journal of Marine Research*, 40, Supplement, 265–290.

Johnson, G. C., Bullister, J. L., & Gruber, N. (2005). Labrador Sea Water property variations in the northeastern Atlantic Ocean. *Geophysical Research Letters*, accepted.

Keeling, R. F., & Garcia, H.E. (2002). The change in oceanic O-2 inventory associated with recent global warming. *Proceedings of the National Academy of Sciences of the United States of America*, 99, 7848-7853.

Keeling, R. F., Piper, S. C., & Heimann, M. (1996). Global and hemispheric CO2 sinks deduced from changes in atmospheric O-2 concentration. *Nature*, 381, 218-221.

Keeling, R. F., & Shertz, S. R. (1992). Seasonal and interannual variations in atmospheric oxygen and implications for the global carbon cycle. *Nature*, 358, 723–727.

Koltermann, K. P., Sokov, A. V., Tereschenkov, V. P., Dobroliubov, S. A., Lorbacher, K., & Sy, A. (1999). Decadal changes in the thermohaline circulation of the North Atlantic. *Deep-Sea Research Part II*, 46, 109–138.

Levitus, S., Antonov, J. I., & Boyer, T. P. (2005). Warming of the World Ocean, 1955-2003. *Geophysical Research Letters*, 32, L02604, doi:10.1029GL021592.

Marshall, J., Johnson, H., & Goodman, J. (2001). A study of the interaction of the North Atlantic Oscillation with ocean circulation. *Journal of Climate*, 14, 1399–1421.

McCartney, M. S., & Talley, L. D. (1982). The Subpolar Mode Water of the North Atlantic Ocean. *Journal of Physical Oceanography*, 12, 1169–1188.

Paillet, J., & Arhan, M., (1996a) Shallow pycnoclines and mode water subduction in the eastern North Atlantic. *Journal of Physical Oceanography*, 26, 2036–2052.

Paillet, J., & Arhan, M., (1996b) Oceanic ventilation in the eastern North Atlantic. *Journal of Physical Oceanography*, 26, 2036–2052.

Pollard, R. T., Griffiths, M. J., Cunningham, S. A., Read, J. F., Perez, F. F., & Rios, A. F. (1996). Vivaldi 1991 – A study of the formation, circulation, and ventilation of Eastern North Atlantic Central Water. *Progress in Oceanography*, 37, 167–192.

Pollard, R. T., Read, J. F., Holliday, N. P., & Leach, H. (2004). Water masses and circulation pathways through the Iceland Basing during Vivaldi 1996. *Journal of Geophysical Research*, 109, C04004, doi:10.1029/2003JC002067.

Potter, R. A., & Lozier, M. S. (2004) On the warming and salinification of the Mediterranean outflow waters in the North Atlantic. *Geophysical Research Letters*, 31, L01202, doi:10.1029/2003GL018161.

Reverdin, G., Assenbaum, M., & Prieur, L. (2005) Eastern North Atlantic mode waters during POMME (September 2000–2001). *Journal of Geophysical Research*, 110, C07S04, doi:10.1029/2004JC002613.

Roemmich, D., & Gould, W. J. (2003). The future of climate observations in the Global Ocean. *Sea Technology*, August, 10–15.

Shaffer, G., Leth, O., Ulloa, O., Bendtsen, J., Daneri, G., Dellarossa, V., Hormazabal, S., & Sehlsted, P.-I. (2000). Warming and circulation change in the eastern South Pacific Ocean. *Geophysical Research Letters*, 27, 1247–1250.

Smythe-Wright, D. (1999). RRS "Discovery" Cruise 233, 23 Apr–01 Jun 1998. A Chemical and Hydrographic Atlantic Ocean Survey: CHAOS. Southampton Oceanography Centre Cruise Report 24, 86 pp.

Tsuchiya, M., Talley, L. D., & McCartney, M. S. (1992). An eastern Atlantic section from Iceland southward across the equator. *Deep-Sea Research Part A*, 39, 1185–1917.

Verbrugge, N., & Reverdin, G. (2003). Contribution of horizontal advection to the interannual variability of sea surface temperature in the North Atlantic. *Journal of Physical Oceanography*, 33, 964–978.

Visbeck, M., Cullen, H., Krahmann, G., & Naik, N. (1998). An ocean model's response to North Atlantic Oscillation – like wind forcing. *Geophysical Research Letters*, 25, 4521–4524.

Volkov, D. L., (2005) Interannual variability of the altimetry-derived eddy field and surface circulation in the extratropical North Atlantic Ocean in 1993–2001, *Journal of Physical Oceanography*, 35, 405–426.

Yashayaev, I., Lazier, J. R. N., & Clarke, R. A. (2003). Temperature and salinity in the central Labrador Sea. *ICES Marine Symposia Series*, 219, 32–39.

Figure Captions

Fig. 1. North Atlantic Oscillation (NAO) index for December – March (DJFM) based on a Principal Component Analysis (PCA) of Sea Level Pressure (SLP) from Hurrell (http://www.cgd.ucar.edu/cas/jhurrell/indices.html). Yearly values (filled bars) are filtered using the backward-looking portion of a 17-point Blackman filter and then advanced by 1 year (solid line) to simulate the effects of ocean circulation memory and lagged response to NAO forcing variations of the few previous winters following Curry and McCartney (2001). Cruise years are marked on the abscissa.

Fig. 2. Station positions (plus signs) for the 2003 reoccupation of World Ocean Circulation Experiment (WOCE) Section A16N along nominal longitude 20°W within the analysis region. Occupations in 1988, 1993, and 1998 are similar, except that the 1993 occupation had roughly doubled distances between stations. Isobaths are contoured at 0 m (thick line) 2000 m (medium line) and 4000 m (thin line).

Fig. 3. Time-mean pressure-latitude sections of water properties along 20°W from repeat occupations of a hydrographic section in 1988, 1993, 1998, and 2003. (a) Potential temperature (θ) contoured at 1.0°C intervals (solid lines) and 0.2°C intervals (dotted lines) below 4°C. (b) Salinity (S) contoured at 0.1 intervals (solid lines) and 0.02 intervals (dotted lines) below 35.0.

Fig. 4. Details follow Fig. 3. (a) Potential vorticity (Q) contoured at 20×10^{-12} m^{-1} s^{-1} intervals (solid lines) and 4×10^{-12} m^{-1} s^{-1} intervals (dotted lines) below 20×10^{-12} m^{-1} s^{-1} with values

below 14×10^{-12} m^{-1} s^{-1} lightly shaded. (b) Apparent Oxygen Utilization (AOU) contoured at 10 μmol kg^{-1} intervals (solid lines).

Fig. 5. Time-mean sections of water properties along 20°W from repeat occupations of a hydrographic section in 1988, 1993, 1998, and 2003. (a) Pressure-latitude section of mean potential density referenced to 1000 dbar (σ_1) contoured at 0.1 kg m^{-3} intervals (solid lines) and 0.02 kg m^{-3} intervals (dotted lines) above 32.3 kg m^{-3}. (b) Potential density (σ_1) -latitude section of pressure (P) contoured at 1000 dbar intervals (solid lines) and 200 dbar intervals shallower than 3000 dbar.

Fig. 6. Time-mean σ_1-latitude sections of water properties along 20°W from repeat occupations of a hydrographic section in 1988, 1993, 1998, and 2003. Near-surface data within the seasonal thermocline (P < 200) dbar) are masked out. (a) Potential temperature (θ) contoured at 1.0°C intervals (solid lines) and 0.2°C intervals (dotted lines) below 4°C. (b) Salinity (S) contoured at 0.1 intervals (solid lines) and 0.02 intervals (dotted lines) below 35.0.

Fig. 7. Details follow Fig. 6. (a) Potential vorticity (Q) contoured at 20×10^{-12} m^{-1} s^{-1} intervals (solid lines) and 4×10^{-12} m^{-1} s^{-1} intervals below 20×10^{-12} m^{-1} s^{-1} with values below 14×10^{-12} m^{-1} s^{-1} lightly shaded. (b) Apparent Oxygen Utilization (AOU) contoured at 10 μmol kg^{-1} intervals (solid lines).

Fig. 8. Latitude-time plot of interannual satellite altimeter sea-surface height anomalies (SSHA) around 20°W (2 cm contour intervals with lower values increasingly shaded) from a merged

gridded product produced by AVISO containing data from multiple satellites (Ducet, Le Traon, & Reverdin, 2000). Latitude-time trajectories of the last three of the four cruises occupied along 20°W and analyzed are indicated (thick solid lines).

Fig. 9. (a, c, and e) Pressure-latitude 2003 - 1993 difference sections of water properties along 20°W with thick positive contours, thin zero and negative contours, and absolute values exceeding the contour interval increasingly shaded. (b, d, and f) Differences of water properties from the mean averaged between 40°N and Iceland. Contour intervals and shading for the sections and axis limits for the difference plots are chosen so that θ and S are scaled according to their relative average contributions to σ_1 in the upper 1500 dbar north of 40°N. For θ (a, b) difference section contours are at 0.5°C intervals. For S (c, d) difference section contours are at 0.107 intervals. For σ_1 (e, f) difference section contours are at 0.083 kg m^{-3} intervals.

Fig. 10. σ_1-latitude 2003 - 1993 difference sections of water properties along 20°W with thick positive contours, thin zero and negative contours, and absolute values exceeding the contour interval increasingly shaded. (a) θ differences contoured at 0.25°C intervals. (b) P differences contoured at 100 dbar intervals.

Fig. 11. (a and c) Pressure-latitude 2003 - 1993 difference sections of water properties along 20°W with thick positive contours, thin zero and negative contours, and absolute values exceeding the contour interval increasingly shaded. (b and d) Differences of water properties from the mean averaged between 40°N and Iceland. For Q (a, b) difference section contours are

at 20×10^{-12} m^{-1} s^{-1} intervals. For AOU (c, d) difference section contours are at 10 μmol kg^{-1} intervals.

Fig. 12. σ_1-latitude 2003 - 1993 difference sections of water properties along 20°W with thick positive contours, thin zero and negative contours, and absolute values exceeding the contour interval increasingly shaded. (a) Q differences contoured at 20×10^{-12} m^{-1} s^{-1} intervals. (b) AOU differences contoured at 10 μmol kg^{-1} intervals.

Fig. 13. Isopycnal average θ-S curves for the 4 occupations of the 20°W section from 45–55°N. Contours of σ_1 at 0.2 kg m^{-3} intervals are overlaid.

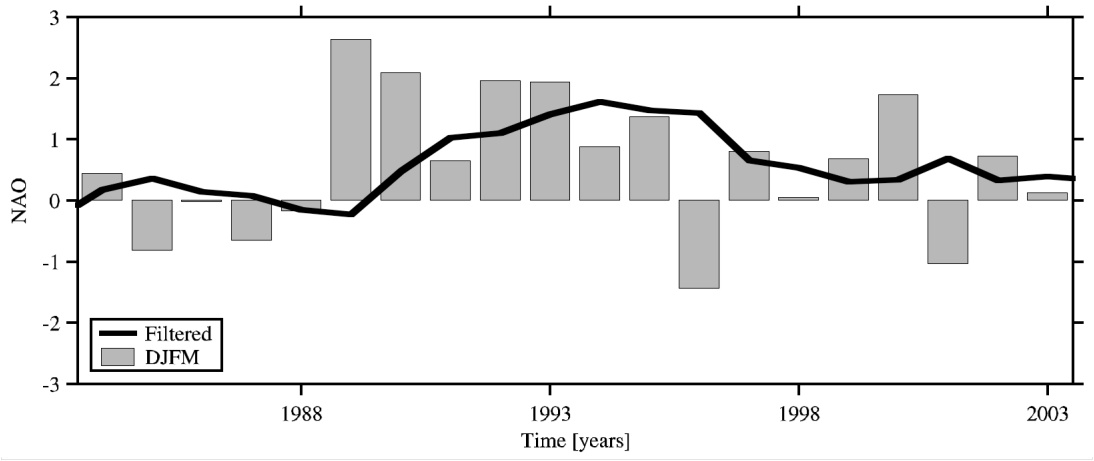

Fig. 1. North Atlantic Oscillation (NAO) index for December – March (DJFM) based on a Principal Component Analysis (PCA) of Sea Level Pressure (SLP) from Hurrell (http://www.cgd.ucar.edu/cas/jhurrell/indices.html). Yearly values (filled bars) are filtered using the backward-looking portion of a 17-point Blackman filter and then advanced by 1 year (solid line) to simulate the effects of ocean circulation memory and lagged response to NAO forcing variations of the few previous winters following Curry and McCartney (2001). Cruise years are marked on the abscissa.

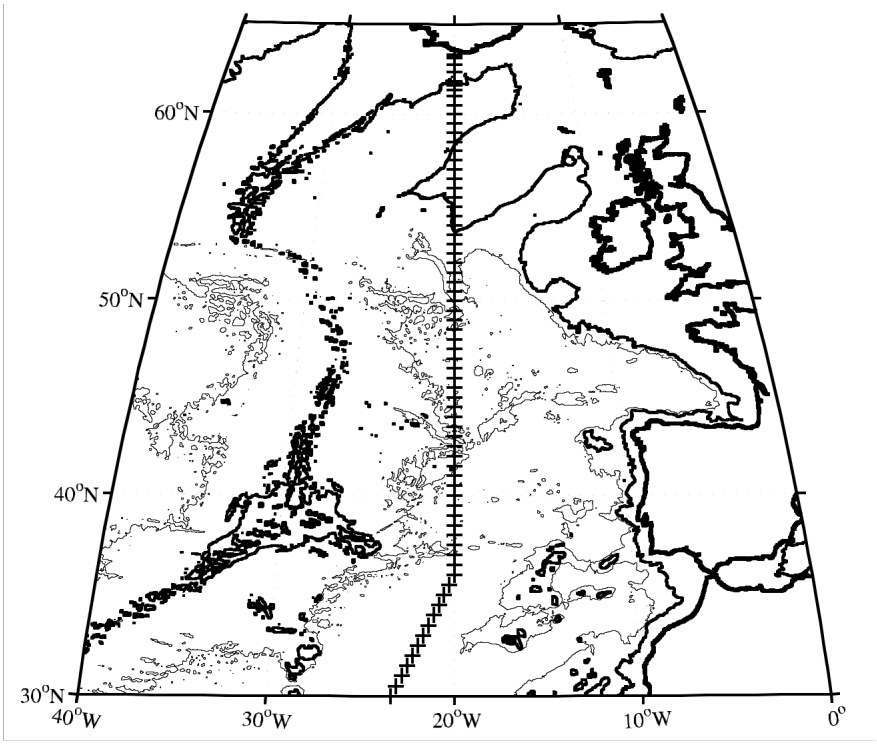

Fig. 2. Station positions (plus signs) for the 2003 reoccupation of World Ocean Circulation Experiment (WOCE) Section A16N along nominal longitude 20°W within the analysis region. Occupations in 1988, 1993, and 1998 are similar, except that the 1993 occupation had roughly doubled distances between stations. Isobaths are contoured at 0 m (thick line) 2000 m (medium line) and 4000 m (thin line).

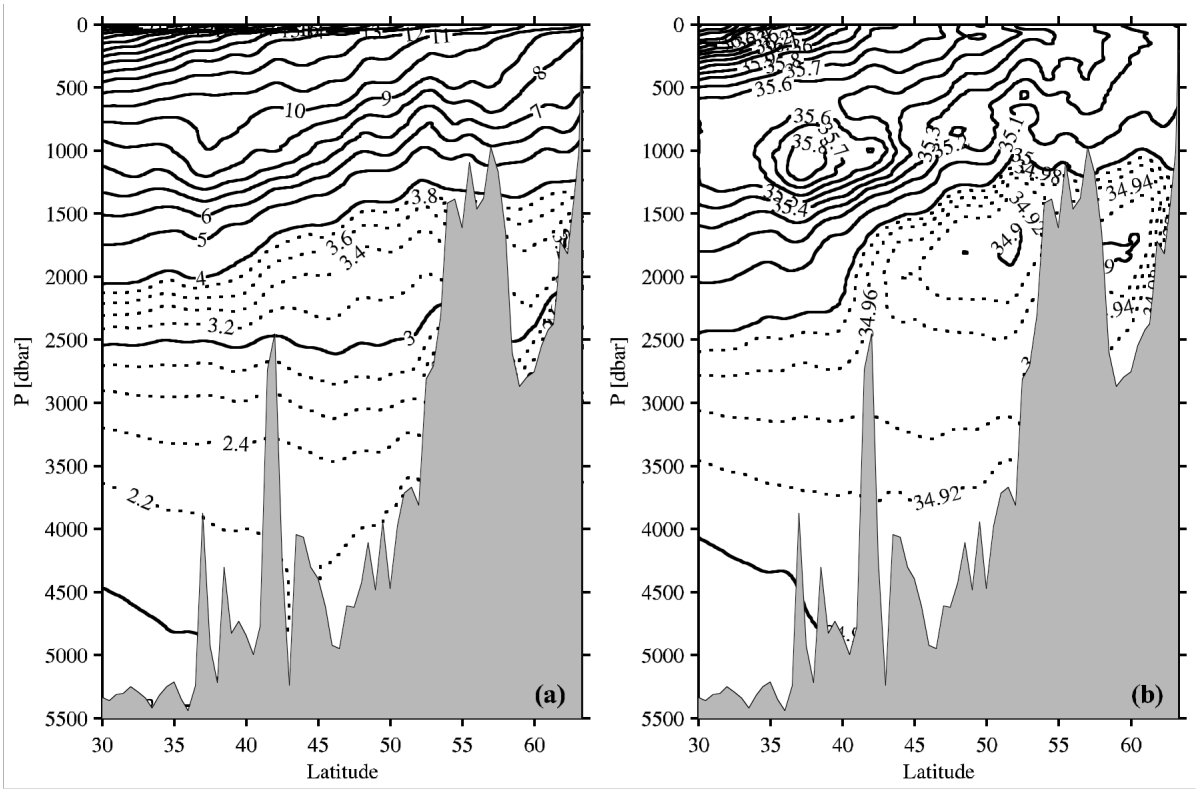

Fig. 3. Time-mean pressure-latitude sections of water properties along 20°W from repeat occupations of a hydrographic section in 1988, 1993, 1998, and 2003. (a) Potential temperature (θ) contoured at 1.0°C intervals (solid lines) and 0.2°C intervals (dotted lines) below 4°C. (b) Salinity (S) contoured at 0.1 intervals (solid lines) and 0.02 intervals (dotted lines) below 35.0.

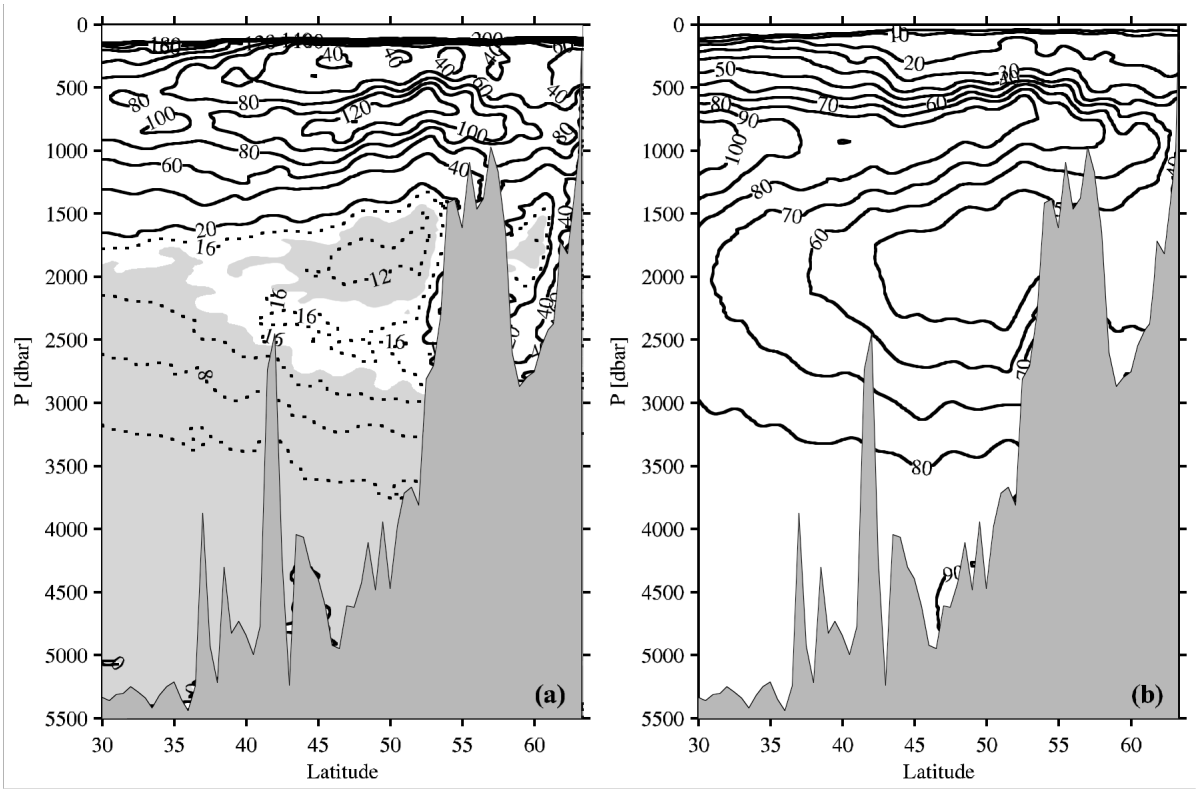

Fig. 4. Details follow Fig. 3. (a) Potential vorticity (Q) contoured at 20×10^{-12} m^{-1} s^{-1} intervals (solid lines) and 4×10^{-12} m^{-1} s^{-1} intervals (dotted lines) below 20×10^{-12} m^{-1} s^{-1} with values below 14×10^{-12} m^{-1} s^{-1} lightly shaded. (b) Apparent Oxygen Utilization (AOU) contoured at 10 μmol kg^{-1} intervals (solid lines).

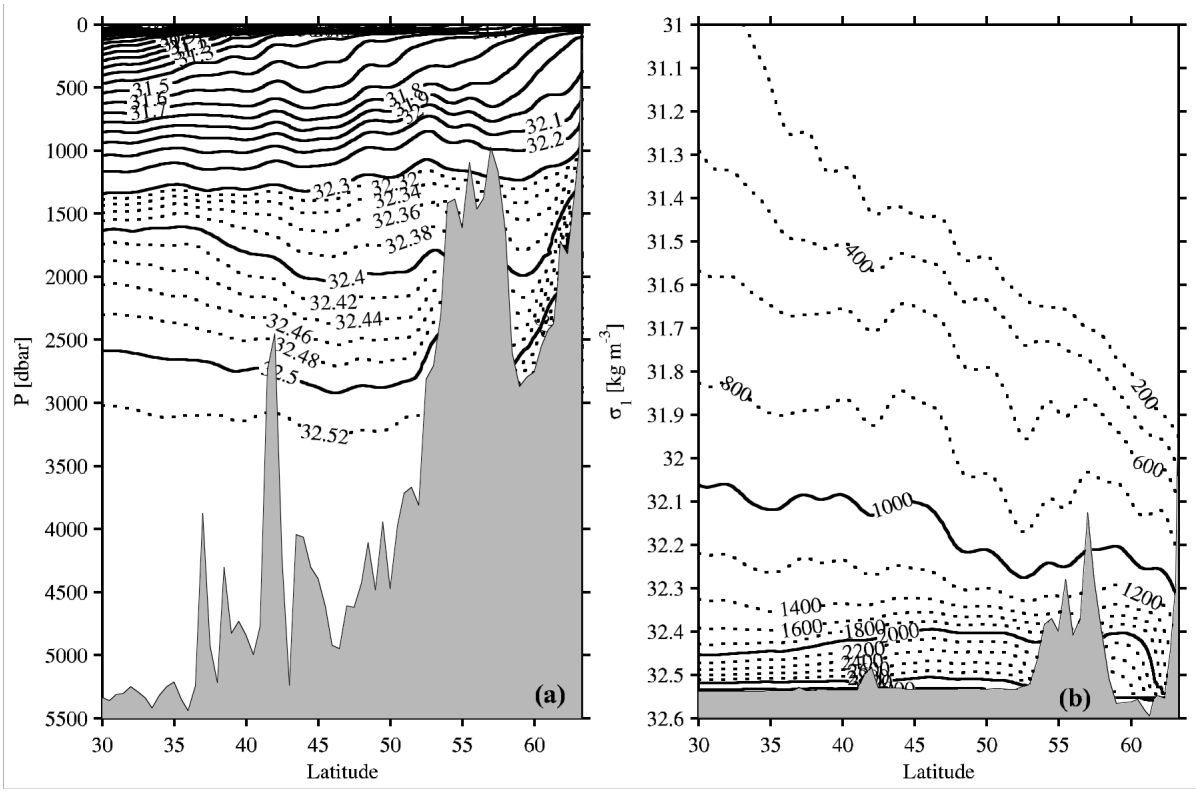

Fig. 5. Time-mean sections of water properties along 20°W from repeat occupations of a hydrographic section in 1988, 1993, 1998, and 2003. (a) Pressure-latitude section of mean potential density referenced to 1000 dbar (σ_1) contoured at 0.1 kg m^{-3} intervals (solid lines) and 0.02 kg m^{-3} intervals (dotted lines) above 32.3 kg m^{-3}. (b) Potential density (σ_1) -latitude section of pressure (P) contoured at 1000 dbar intervals (solid lines) and 200 dbar intervals shallower than 3000 dbar.

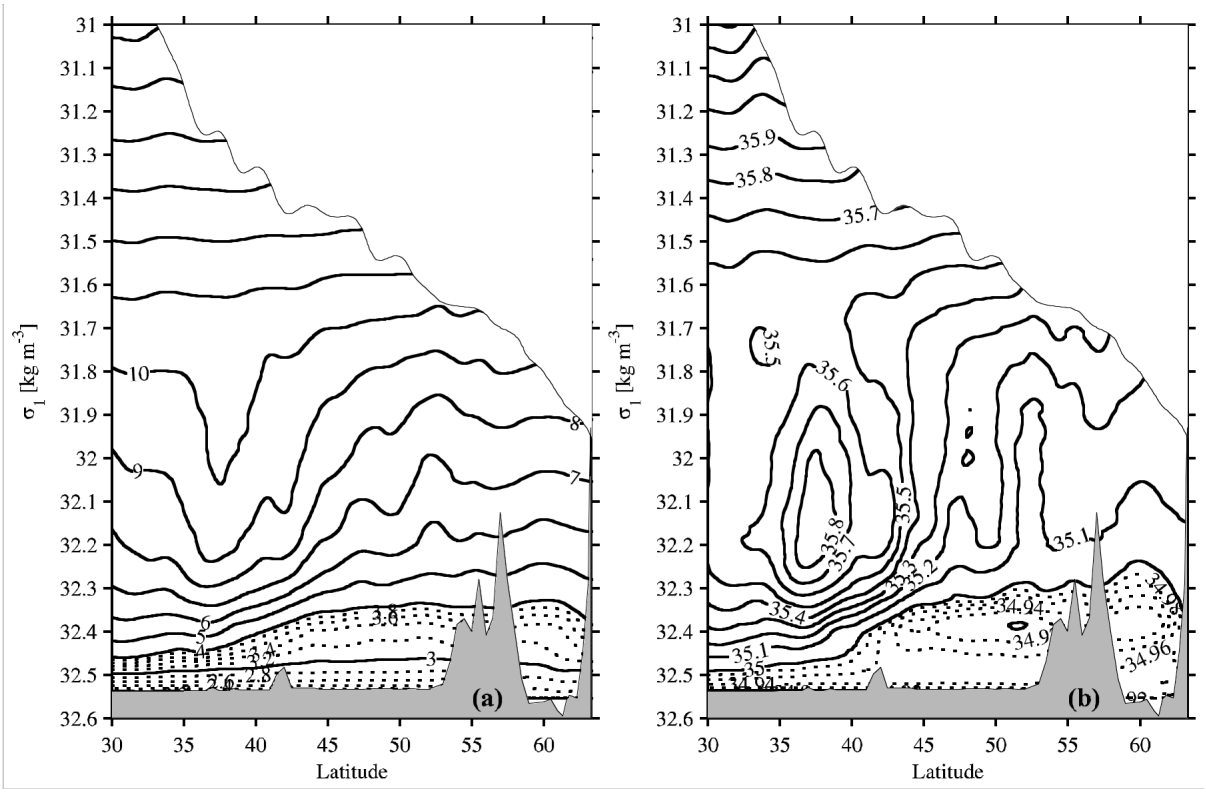

Fig. 6. Time-mean σ_1-latitude sections of water properties along 20°W from repeat occupations of a hydrographic section in 1988, 1993, 1998, and 2003. Near-surface data within the seasonal thermocline (P < 200) dbar) are masked out. (a) Potential temperature (θ) contoured at 1.0°C intervals (solid lines) and 0.2°C intervals (dotted lines) below 4°C. (b) Salinity (S) contoured at 0.1 intervals (solid lines) and 0.02 intervals (dotted lines) below 35.0.

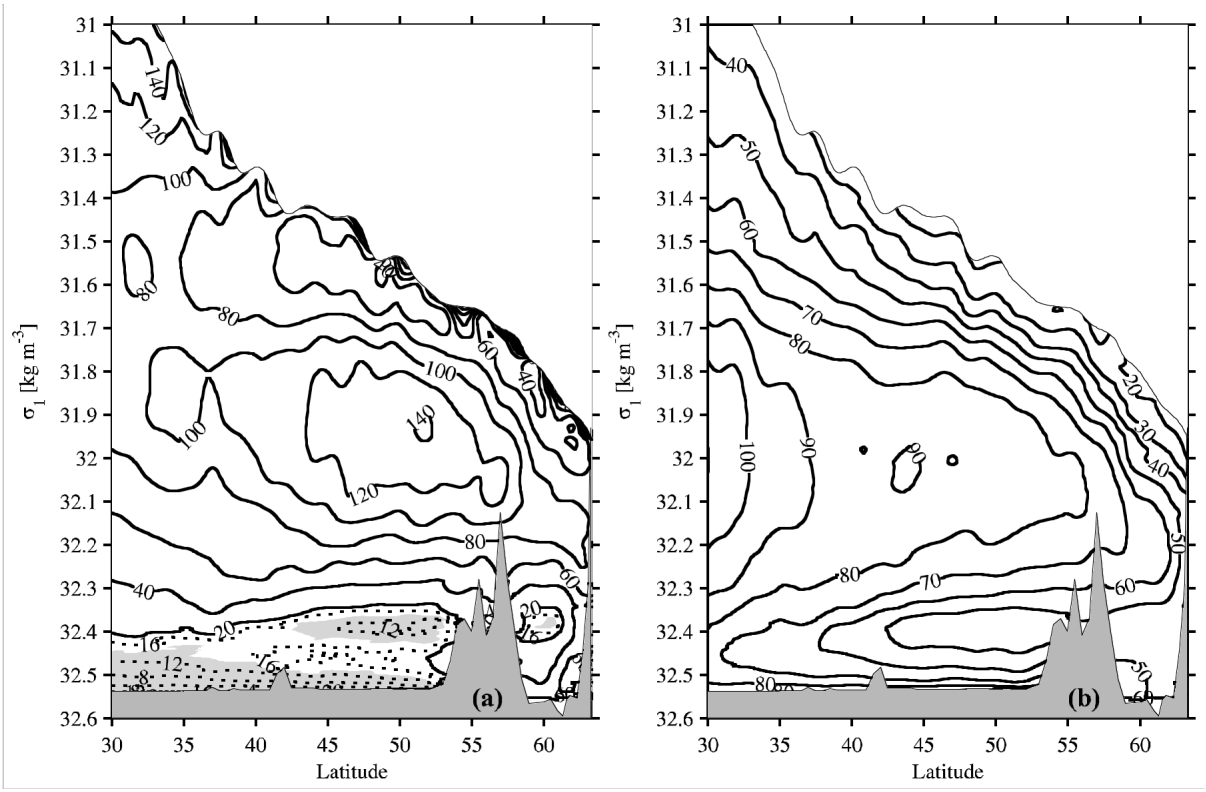

Fig. 7. Details follow Fig. 6. (a) Potential vorticity (Q) contoured at 20×10^{-12} m^{-1} s^{-1} intervals (solid lines) and 4×10^{-12} m^{-1} s^{-1} intervals below 20×10^{-12} m^{-1} s^{-1} with values below 14×10^{-12} m^{-1} s^{-1} lightly shaded. (b) Apparent Oxygen Utilization (AOU) contoured at 10 μmol kg^{-1} intervals (solid lines).

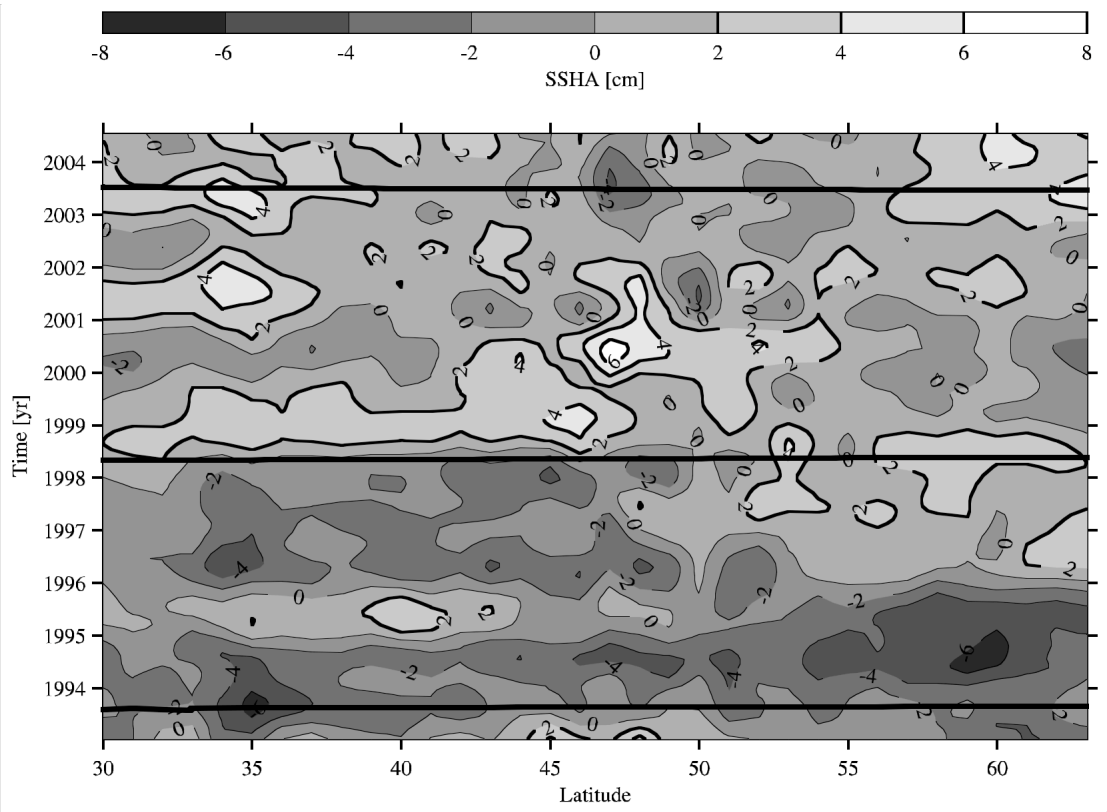

Fig. 8. Latitude-time plot of interannual satellite altimeter sea-surface height anomalies (SSHA) around 20°W (2 cm contour intervals with lower values increasingly shaded) from a merged gridded product produced by AVISO containing data from multiple satellites (Ducet, Le Traon, & Reverdin, 2000). Latitude-time trajectories of the last three of the four cruises occupied along 20°W and analyzed are indicated (thick solid lines).

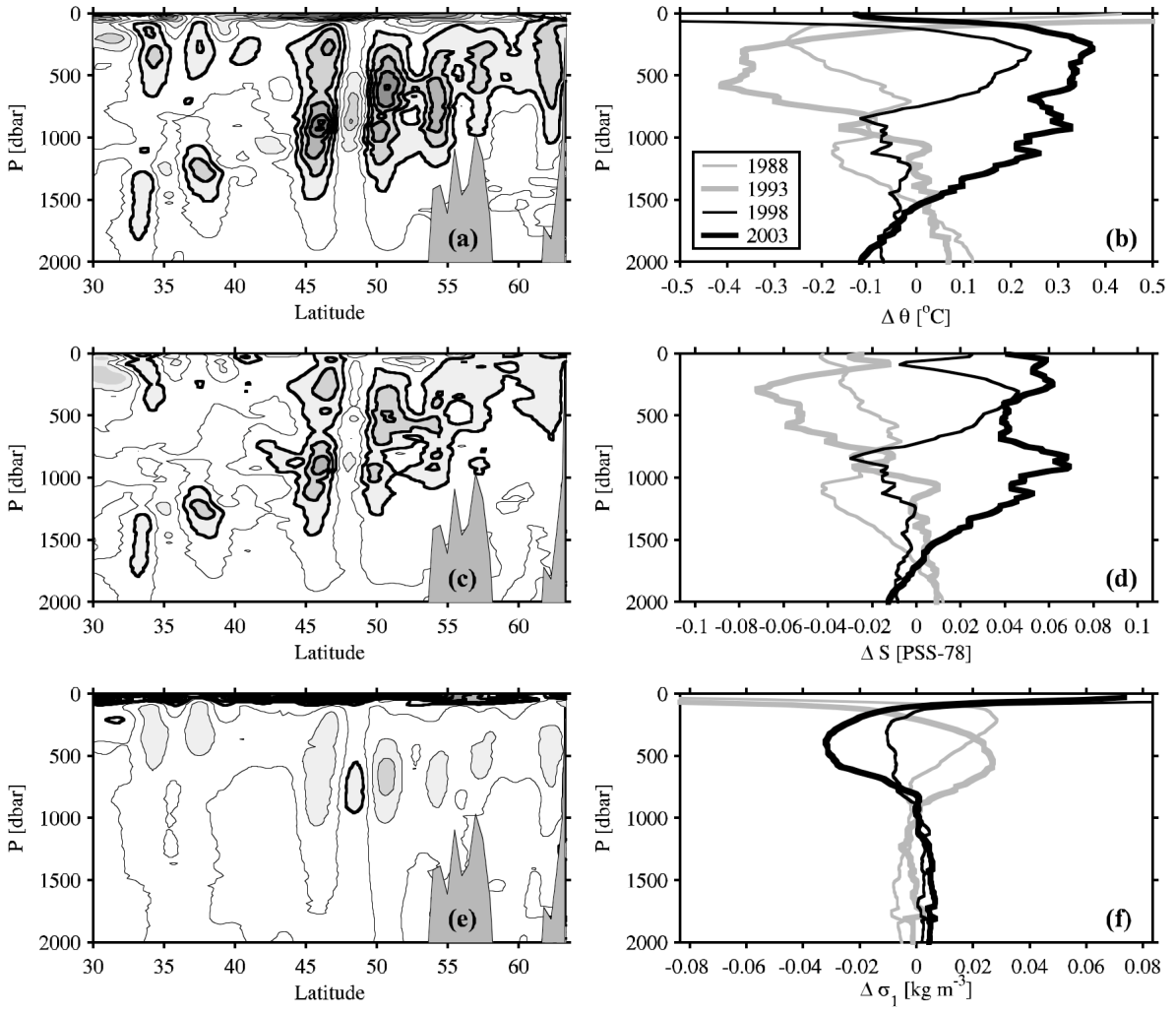

Fig. 9. (a, c, and e) Pressure-latitude 2003 - 1993 difference sections of water properties along 20°W with thick positive contours, thin zero and negative contours, and absolute values exceeding the contour interval increasingly shaded. (b, d, and f) Differences of water properties from the mean averaged between 40°N and Iceland. Contour intervals and shading for the sections and axis limits for the difference plots are chosen so that θ and S are scaled according to their relative average contributions to σ_1 in the upper 1500 dbar north of 40°N. For θ (a, b) difference section contours are at 0.5°C intervals. For S (c, d) difference section contours are at 0.107 intervals. For σ_1 (e, f) difference section contours are at 0.083 kg m^{-3} intervals.

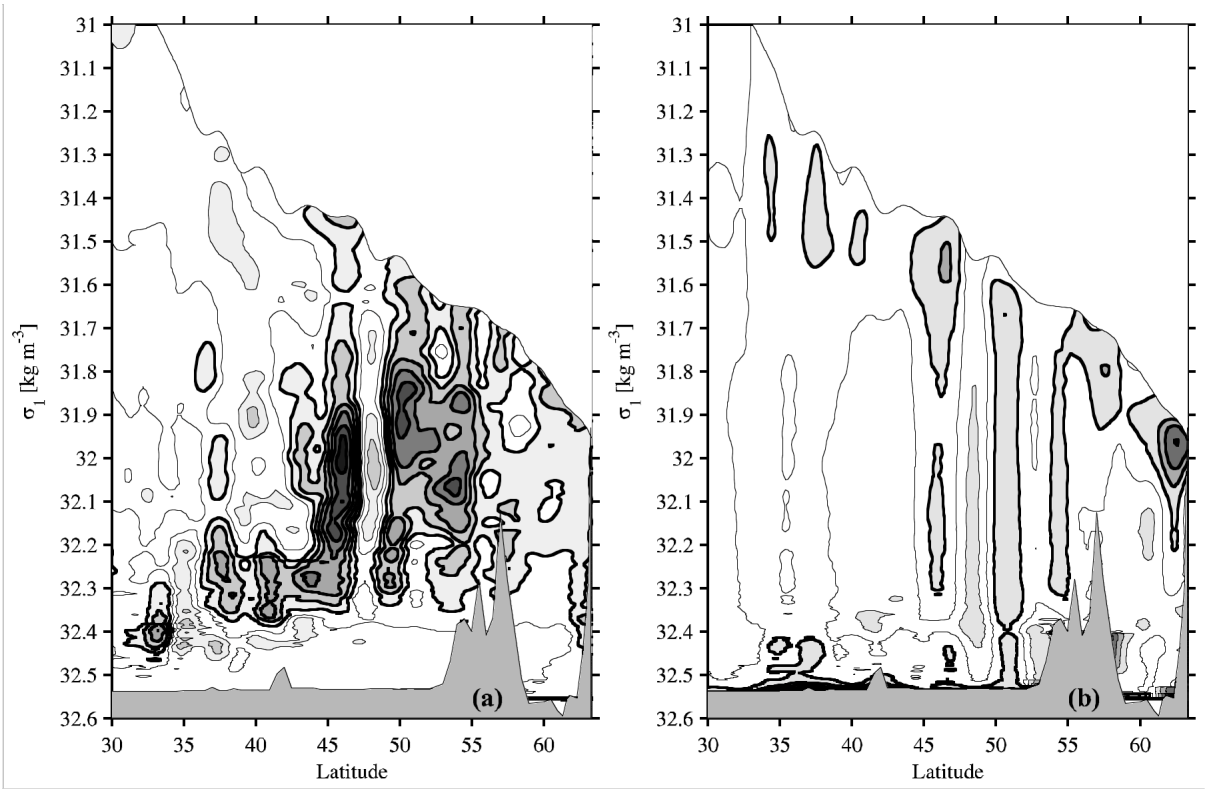

Fig. 10. σ_l-latitude 2003 - 1993 difference sections of water properties along 20°W with thick positive contours, thin zero and negative contours, and absolute values exceeding the contour interval increasingly shaded. (a) θ differences contoured at 0.25°C intervals. (b) P differences contoured at 100 dbar intervals.

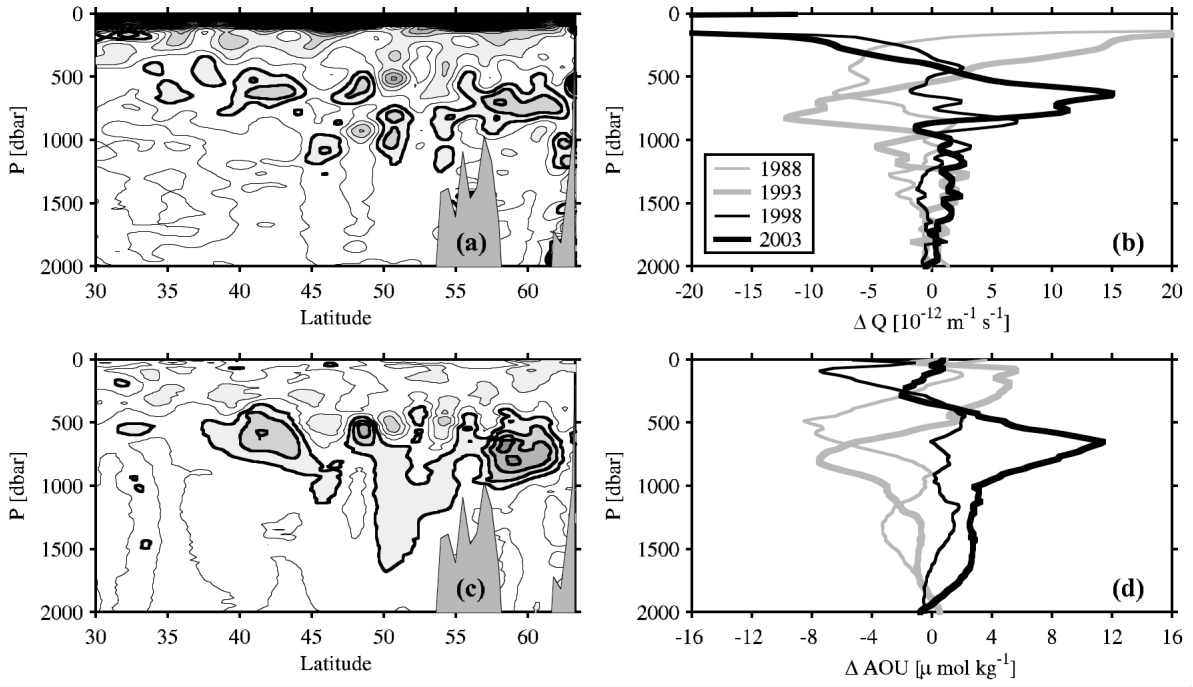

Fig. 11. (a and c) Pressure-latitude 2003 - 1993 difference sections of water properties along 20°W with thick positive contours, thin zero and negative contours, and absolute values exceeding the contour interval increasingly shaded. (b and d) Differences of water properties from the mean averaged between 40°N and Iceland. For Q (a, b) difference section contours are at 20×10^{-12} m^{-1} s^{-1} intervals. For AOU (c, d) difference section contours are at 10 μmol kg^{-1} intervals.

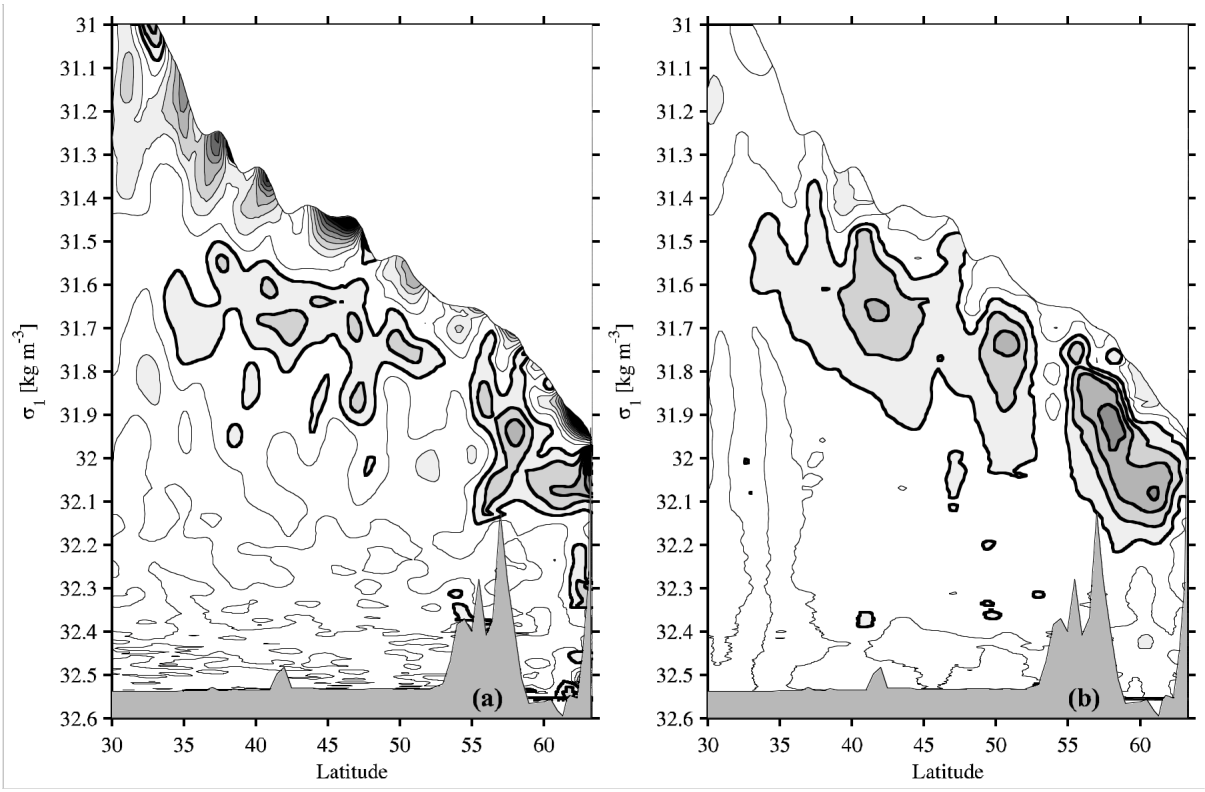

Fig. 12. σ_1-latitude 2003 - 1993 difference sections of water properties along 20°W with thick positive contours, thin zero and negative contours, and absolute values exceeding the contour interval increasingly shaded. (a) Q differences contoured at 20×10^{-12} m^{-1} s^{-1} intervals. (b) AOU differences contoured at 10 μmol kg^{-1} intervals.

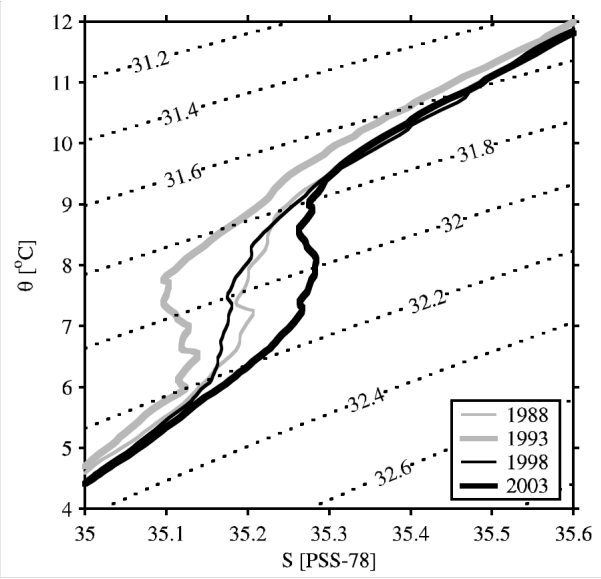

Fig. 13. Isopycnal average θ-S curves for the 4 occupations of the 20°W section from 45–55°N. Contours of σ_1 at 0.2 kg m^{-3} intervals are overlaid.